THE JOURNAL OF BIOLOGICAL CHEMISTRY VOL. 287, NO. 10, pp. 7279–7288, March 2, 2012

Heteromeric Heat-sensitive Transient Receptor Potential Channels Exhibit Distinct Temperature and Chemical Response*

Received for publication, September 16, 2011, and in revised form, December 7, 2011 Published, JBC Papers in Press, December 19, 2011, DOI 10.1074/jbc.M111.305045

Wei Cheng[‡§1], **Fan Yang**[§¶1], **Shuang Liu**[‖], **Craig K. Colton**[**], **Chunbo Wang**[**], **Yuanyuan Cui**[§‖], **Xu Cao**[§‖], **Michael X. Zhu**[‡‡], **Changsen Sun**[‡], **KeWei Wang**[‖2], **and Jie Zheng**[§3]

From the [‡]*Laboratory of Biomedical Optics, College of Physics and Optoelectronic Engineering, Dalian University of Technology, Dalian 116023, China, the* [§]*Department of Physiology and Membrane Biology and* [¶]*Molecular, Cellular, and Integrative Physiology Graduate Group, University of California, Davis, California 95616, the* [‖]*Department of Neurobiology, Neuroscience Research Institute, Peking University Health Science Center, Beijing 100083, China, the* [**]*Center for Molecular Neurobiology, Ohio State University, Columbus, Ohio 43210, and the* [‡‡]*Department of Integrative Biology and Pharmacology, University of Texas Health Science Center, Houston, Texas 77030*

Background: TRPV1 and TRPV3 subunits are known to form heteromeric channels with unknown functional properties.
Results: Heteromeric TRPV1/TRPV3 channels exhibit unique activation threshold temperature, dynamic range, potentiation to repetitive heating, and capsaicin sensitivity.
Conclusion: Heteromeric channels are unique sensors for heat and chemical stimuli.
Significance: Heteromeric channels may contribute to the fine-tuning of human sensitivity to sensory inputs.

TRPV1 and TRPV3 are two heat-sensitive ion channels activated at distinct temperature ranges perceived by human as hot and warm, respectively. Compounds eliciting human sensations of heat or warmth can also potently activate these channels. In rodents, TRPV3 is expressed predominantly in skin keratinocytes, whereas in humans TRPV1 and TRPV3 are co-expressed in sensory neurons of dorsal root ganglia and trigeminal ganglion and are known to form heteromeric channels with distinct single channel conductances as well as sensitivities to TRPV1 activator capsaicin and inhibitor capsazepine. However, how heteromeric TRPV1/TRPV3 channels respond to heat and other stimuli remains unknown. In this study, we examined the behavior of heteromeric TRPV1/TRPV3 channels activated by heat, capsaicin, and voltage. Our results demonstrate that the heteromeric channels exhibit distinct temperature sensitivity, activation threshold, and heat-induced sensitization. Changes in gating properties apparently originate from interactions between TRPV1 and TRPV3 subunits. Our results suggest that heteromeric TRPV1/TRPV3 channels are unique heat sensors that may contribute to the fine-tuning of sensitivity to sensory inputs.

TRPV1 and TRPV3 are two members of the vanilloid receptor branch of the transient receptor potential channels, TRPVs,[4] that serve as cellular sensors for increases in temperature and the presence of pungent chemical stimuli (1–4). They are Ca^{2+}-permeable nonselective cation channels with a similar structural architecture (5). Like voltage-dependent potassium channels, they are tetramers with four subunits surrounding a centrally located ion-conducting pore (6). Each subunit has six transmembrane segments, with the last two transmembrane segments and the linker between them forming the ion permeation pore. TRPV1 and TRPV3 subunits exhibit about 50% overall sequence similarity, and the similarity between the transmembrane regions is much higher. They also share a number of functional domains, such as the intracellular N-terminal ankyrin-like repeats domain (7, 8) and the charged amino acid-rich TRP domain located proximal to the S6 transmembrane segment (9).

Despite structural similarity, TRPV1 and TRPV3 show distinct functional properties. TRPV1 is strongly activated by temperatures above 40 °C and by capsaicin (CAP) (10–12). TRPV3 is activated at much lower temperatures (~30 °C) and by chemicals such as camphor, vanillin, carvocral, and cinnamaldehyde that elicit warm sensation (13–17). In addition, the kinetics of temperature response by TRPV1 and TRPV3 are very different, whereas TRPV1 is activated rapidly by brief elevation to high temperatures, TRPV3 activates at a much slower pace. Furthermore, TRPV1 can be desensitized by prolonged or repetitive heating, whereas TRPV3 exhibits prominent sensitization to repetitive heating (15). These differences in gating properties are expected to have profound impact on their physiological roles as temperature and pain sensors.

* This work was supported, in whole or in part, by National Institutes of Health Grants NS072377 (to J. Z.) and GM081658 (to M. X. Z.). This work was also supported by the University of California Davis Health System (to J. Z.), National Science Foundation of China Grants 30970919 (to K. W. W.) and 3092800 (to J. Z.), Ministry of Education of China 111 Project B07001 (to K. W. W.), and an American Heart Association predoctoral fellowship (to F. Y.).

[1] Both authors contributed equally to this work.
[2] To whom correspondence may be addressed. E-mail: wangkw@bjmu.edu.cn.
[3] To whom correspondence may be addressed. E-mail: jzheng@ucdavis.edu.

[4] The abbreviations used are: TRPV, transient receptor potential vanilloid; TRP, transient receptor potential; CAP, capsaicin; eYFP, enhanced yellow fluorescent protein; CZP, capsazepine; RR, ruthenium red; DRG, dorsal root ganglion.

TRPV1 and TRPV3 are encoded by genes located adjacent to each other in the human and mouse genomes (13–15). In human and non-human primates, expression of both TRPV1 and TRPV3 in sensory neurons is detected at mRNA and protein levels (14, 15, 18). However, in rodents (*e.g.* rat and mouse) TRPV3 is found to express predominantly in keratinocytes (13). The difference in tissue distribution calls for caution in interpreting the applicability of behavior and knock-out studies in rodents to human physiology (19, 20). Indeed, it was previously found that TRPV1 and TRPV3 subunits co-assemble into heteromeric channels (14, 21). Like other heteromeric TRP channels (22), heteromeric TRPV1/TRPV3 channels exhibit single channel conductances and chemical sensitivity that are distinct from the homomeric channels (21). However, very little is known about the functional properties of the heteromeric channels. In particular, how heteromeric TRPV channels respond to temperature remains unknown. Given the dramatic functional differences between TRPV1 and TRPV3 homomeric channels, it is of great interest to understand how heteromeric channels formed between them preserve the physiological properties of each subunit type and respond to benign or noxious stimuli. In this study, we use electrophysiological and fluorescence microscopic recordings to demonstrate that heteromeric TRPV1/TRPV3 channels exhibit unique temperature and chemical responses.

MATERIALS AND METHODS

Molecular Biology and Cell Culture—Mouse TRPV1 and TRPV3 cDNAs were fused at the C-terminal end to a cDNA encoding either cerulean (a brighter version of the enhanced cyan fluorescent protein) or the enhanced yellow fluorescent protein (eYFP), as described previously (21). The fluorescent tag facilitated identification of positively transfected cells but did not significantly alter channel function (21). A TRPV1-TRPV3 concatemer was described previously (23), in which the C terminus of TRPV1 was linked to the N terminus of TRPV3 by a short amino acid chain (CQQQQFCSRAQASNSAVDD). No fluorescent protein tag was used in the concatemer. We have previously confirmed with a TRPV1-TRPV1 concatemer that covalent linkage did not exert a detectable effect on channel function (24). All constructs were confirmed by sequencing.

HEK293 cells were plated at low densities and allowed to grow overnight in Dulbecco's modified Eagle's medium (DMEM) supplemented with 20 mM L-glutamine and 10% FBS. Cells were transiently transfected using Lipofectamine 2000 (Invitrogen) following standard protocols. After 1–2 days, expressed cells were chosen to perform patch clamp recording. For TRPV1 + TRPV3 co-expression experiments, cells exhibiting strong fluorescence from both cerulean and eYFP were selected. For TRPV1-TRPV3 concatemer, eYFP was co-transfected with the concatemer at a ratio of ~1:4. Cells that showed significant eYFP fluorescence were selected.

Electrophysiology—Patch clamp recordings were done using an EPC10 amplifier driven by the PatchMaster software (HEKA) in the cell-free inside-out or whole-cell configuration. For both configurations, the bath solution and the pipette solution contained (in mM) the following: 130 NaCl, 3 HEPES, and 0.2 EDTA (pH 7.2). All recordings were done at room temperature unless specified; the variation in temperature in these experiments, monitored by a thermistor placed next to the patch pipette, in most cases was within 1 °C. Capsaicin or capsazepine was applied to the patch with a rapid solution changer (RSC-200, Bio-Logic). The speed of solution exchange was estimated by monitoring the time course of junction potential change that occurred at the tip of an open pipette. Solution exchange was always completed within 100 ms. EC_{50} or IC_{50} was derived from fitting the dose-response relationship to a Hill equation. Rates of current inhibition and recovery were estimated by fitting the time course to a single exponential function. *G-V* curves were fitted to a single Boltzmann function as shown in Equation 1,

$$G/G_{max} = \frac{1}{1 + \exp(-qF(V - V_{half})/RT)} \quad \text{(Eq. 1)}$$

from which the half-activation voltage, V_{half}, and the apparent gating charge, q, were estimated. A single exponential function was used to fit the latter part of depolarization-induced current to estimate the activation rate; similarly, a single exponential function was fitted to the hyperpolarizing voltage-induced channel closure to evaluate the deactivation rate. All statistical data are given as mean ± S.E. Student's *t* test was used to examine the significance of statistical differences.

Ca^{2+} Imaging—Transiently transfected HEK293 cells seeded in 96-well plates were washed once with an extracellular solution containing 140 mM NaCl, 5 mM KCl, 1 mM $MgCl_2$, 1.8 mM $CaCl_2$, 10 mM glucose, and 15 mM HEPES (pH 7.4) and then incubated in 50 μl of extracellular solution supplemented with 2 μM fluo-4/AM and 0.05% Pluronic F-127 (both were from Molecular Probes, Eugene, OR) at 37 °C for 60 min. Probenecid (2 mM) was included in all of the solutions to prevent fluo-4 leakage from cells. At the end of the incubation, the cells were washed three times with extracellular solution and placed in 80 μl of the same solution. Intracellular Ca^{2+} was measured using a fluid-handling integrated fluorescence plate reader (Flex Station, Molecular Devices, Sunnyvale, CA). Capsaicin and other drugs were diluted into extracellular solution at three times the desired final concentrations and delivered to the sample plate by the integrated robotic eight-channel pipettor at the preprogrammed time points. The fluo-4 fluorescence was read at an excitation wavelength of 494 nm and emission wavelength of 525 nm from the bottom of the plate at 0.67 Hz. All of the experiments were performed at 32 °C.

Temperature Control—Temperature control was achieved in two ways as follows: 1) perfusion of pre-heated or pre-cooled solution; 2) heating by infrared laser irradiation. For the perfusion-based method, reservoirs were placed about 20 cm above the recording chamber, and solution flow was driven by gravity. Heating of solutions was done with an SHM-828 multiple line heater controlled by a CL-100 temperature controller (Harvard Apparatus). Up to eight solutions were heated simultaneously via separated lines. A custom-made manifold was attached to the output ports of the heater. Solution cooling was achieved by perfusing a cooled solution, which was embedded in ice water, through a separate line into the recording chamber. The patch pipette was placed about 1 mm from the solution output ports. A TA-29 miniature bead thermistor (Harvard Apparatus) was

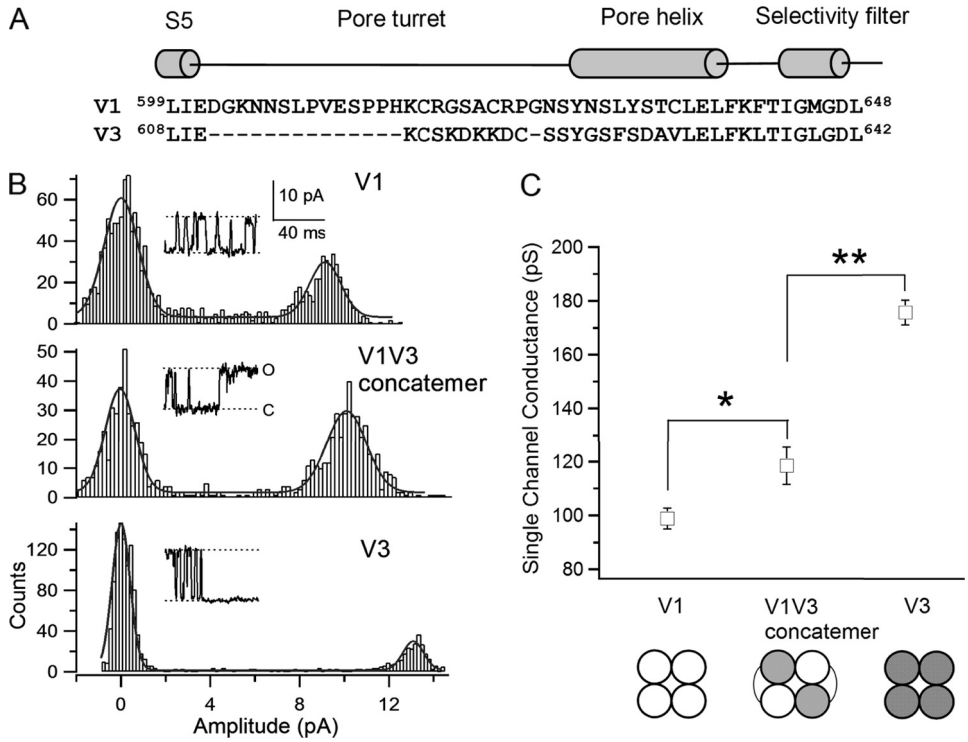

FIGURE 1. **Heteromeric TRPV1/TRPV3 channels exhibit intermediate single channel conductance.** *A*, sequence alignment between the pore regions of TRPV1 and TRPV3. *B*, representative single channel current traces recorded from cells expressing TRPV1, TRPV3, or TRPV1-TRPV3 concatemer at +80 mV. All-point histograms of current amplitude for each channel type are superimposed with fits of a double-Gaussian function. *C*, single channel conductance of TRPV1/TRPV3 concatemers (118.6 ± 6.9 picosiemens (*pS*), $n = 6$) is between those of homomeric TRPV1 (99.0 ± 3.9 picosiemens ($n = 6$) and TRPV3 (175.7 ± 4.6 picosiemens, $n = 4$) determined at +80 mV. *, $p < 0.05$; **, $p < 0.01$.

placed right next to (<1 mm) the pipette to ensure accurate monitoring of local temperature. Temperature readout by the thermistor was fed into an analog input port of the EPC10 patch clamp amplifier and recorded simultaneously with current.

Perfusion-based heating was applied for steady state measurement of threshold temperature. Solution flow was turned on first, and the heater was set to the desired temperature. In this way, the temperature changing rate was low (at about 0.15 °C/s) to ensure that the temperature-driven transition was at equilibrium. The current-temperature relationship exhibited two phases, a slow increase (probably representing the temperature-dependent increase in leak current) followed by a rapid takeoff phase. A linear fit was done for each of these two phases. The intersect point of the two fitting lines was defined as the threshold temperature.

To characterize heat-induced activation kinetics, a rapid laser heating approach was used (25). Briefly, a 1443-nm laser diode (Fitel) with controllers (Thorlabs) was used to generate a continuous narrow laser beam. The maximum optic output power was 250 milliwatts. The core diameter of laser-conducting optic fiber was 10 μm. The patch pipette tip was placed right in front of the center of optic fiber open end. When the laser was turned on, light energy was efficiently absorbed by water and converted to heat, elevating the local temperature rapidly.

To calibrate the laser heating system, the solution temperature of the bath chamber was held at constant levels by pumping heated water that circulated around the chamber. An open glass pipette filled with a solution distinct from the bath solution was immersed in the chamber. A thermistor as described above was placed next to the open pipette. In this way the junction potential at different temperatures was measured. Subsequently, the same pipette was centered at the end of the laser optic fiber. The laser driving power was adjusted to produce junction potential values matching those measured at different temperatures. In this way, the relationship between laser driving power and temperature was tabulated.

To determine the rate of laser-induced heating, again an open pipette was centered at the end of the laser optic fiber. The rate of junction potential change in response to a particular laser power was recorded. In this way, it was determined that the temperature at the pipette tip can reach 45 °C within 30 ms. To measure the rate of heat-induced channel activation, a single exponential function was fitted to the rising phase of the current response to estimate the time constant. Because the current response of TRPV3 and heteromers could be dramatically potentiated upon repeated heating, all kinetic analyses were done with the first heating response.

To calculate the activation energy (E_a), time constants of heat activation measured in response to different temperatures were first converted to the natural log form before plotted against the inverse of temperature. The Arrhenius Equation 2 was used to fit the data set,

$$\ln(\tau) = \frac{E_a}{R \cdot T} + \ln(A) \qquad \text{(Eq. 2)}$$

where R is the gas constant; T is the temperature in Kelvin, and A is a prefactor. E_a was estimated from the slope of the fitted line.

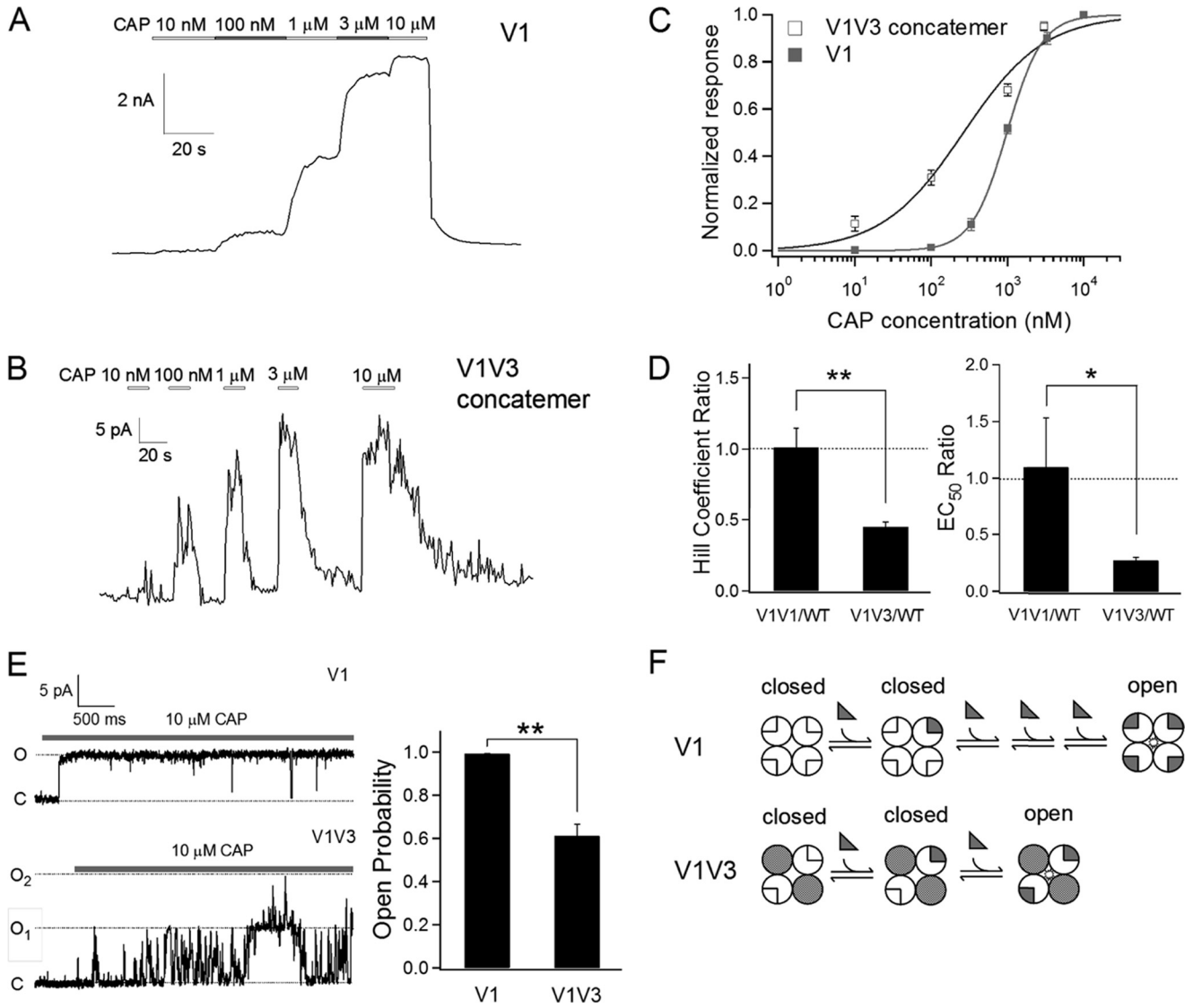

FIGURE 2. **Heteromeric TRPV1/TRPV3 channels exhibit altered capsaicin sensitivity.** *A* and *B*, representative current traces of TRPV1 (*A*) and TRPV1/TRPV3 concatemer (*B*), recorded at +80 mV in response to different concentrations of capsaicin. *C*, capsaicin dose-response curves of TRPV1/TRPV3 (*open squares*) and TRPV1 (*filled squares*). The *curves* represent fits to the Hill equation. The EC_{50} and slope factor values are as follows: 269 ± 27 nM and 0.85 ± 0.06 ($n = 6$) for TRPV1/TRPV3; 981 ± 59 nM and 1.88 ± 0.07 ($n = 3$) for TRPV1. *D*, comparison of Hill coefficient (*left panel*) and EC_{50} (*right panel*) of TRPV1-TRPV1 and TRPV1-TRPV3 channels (normalized to TRPV1, $n = 6$ each). *E*, example of single channel traces of TRPV1 and TRPV1-TRPV3 channels in response to 10 μM capsaicin (*left panel*). The *bar graph* represents mean open probability values ($n = 3$ for TRPV1; $n = 4$ for TRPV1-TRPV3). *F*, model of capsaicin activation. *Gray triangles* represents capsaicin molecule. TRPV1 subunits are illustrated as *open circles*, and TRPV3 subunits are shown as *hatched circles*. *, $p < 0.05$; **, $p < 0.01$.

RESULTS

Formation of Functional Heteromeric TRPV1/TRPV3 Channels—Previously, we have demonstrated that co-expressing TRPV1 and TRPV3 subunits yielded heteromeric channels of random subunit stoichiometries (21). Reflecting the difference in sequence of their pore regions (Fig. 1*A*), these heteromeric channels exhibited intermediate single channel conductances comparing with the homomeric TRPV1 and TRPV3 channels. To characterize functional properties of a single population of heteromeric TRPV1/TRPV3 channels, in this study we made use of a concatemer approach (26) in which the cDNA for TRPV1 was covalently linked with that for TRPV3 in a single expression vector (23). Expressing this concatemer construct yielded heteromeric channels with two TRPV1 subunits and two TRPV3 subunits in alternate positions (Fig. 1*C*).

To first confirm that the TRPV1-TRPV3 concatemer vector indeed produced a single population of heteromeric TRPV1/TRPV3 channels, we employed inside-out patch clamping to record single channels from the concatemer-expressing cells. Indeed, the single channel conductance exhibited a uniform intermediate value between those of homomeric TRPV1 and TRPV3 (Fig. 1, *B* and *C*). This observation is in agreement with our previous findings from TRPV1 + TRPV3 co-expression (21). Therefore, by either co-expressing TRPV1 and TRPV3 or expressing the TRPV1-TRPV3 concatemer, we were able to generate functional heteromeric TRPV1/TRPV3 channels on the cell membrane.

Altered Ligand Gating of Heteromeric TRPV1/TRPV3 Channels—Capsaicin (CAP) is a highly specific agonist for TRPV1 that exerts no effect on TRPV3. We found that the

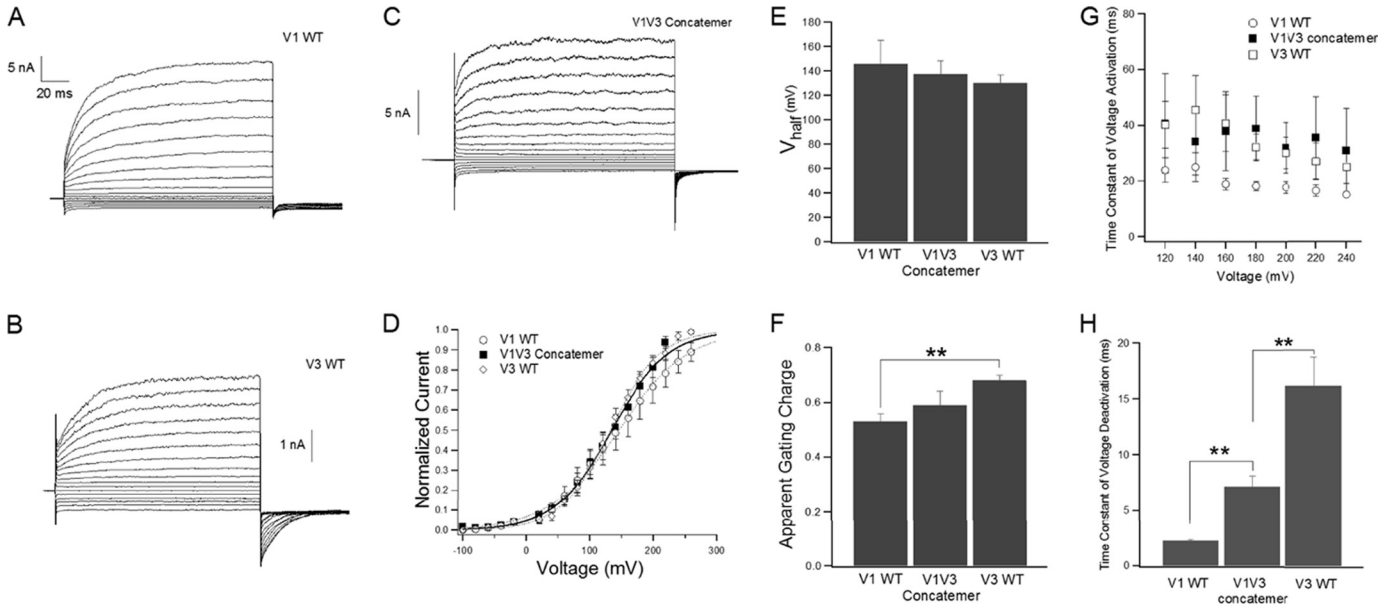

FIGURE 3. **Voltage dependence properties of homomeric TRPV1, TRPV3, and heteromeric TRPV1/TRPV3 channel.** *A–C,* representative macroscopic currents from TRPV1, TRPV3, and TRPV1-TRPV3 concatemer in response to voltage steps to −100 to +220 mV for 150 ms from a holding potential of 0 mV. *D, G-V* curves fitted to a Boltzmann function. For homomeric TRPV1, $V_{half} = 146 \pm 19$ mV, $q = 0.53 \pm 0.03\ e_0$ ($n = 5$); for homomeric TRPV3, $V_{half} = 130 \pm 7$ mV, $q = 0.68 \pm 0.02\ e_0$ ($n = 7$); for TRPV1-TRPV3 concatemer, $V_{half} = 138 \pm 11$ mV, $q = 0.59 \pm 0.05\ e_0$ ($n = 7$). *E*, comparison of the V_{half} values. *F*, comparison of the apparent gating charge *q* values. *G*, time constants of voltage-dependent activation of homomeric TRPV1 ($n = 4$), TRPV3 ($n = 3$–5), and TRPV1-TRPV3 concatemer ($n = 5$–7) measured at different voltages. *H*, time constants of voltage-dependent deactivation of homomeric TRPV1 ($n = 4$), TRPV3 ($n = 5$), and TRPV1-TRPV3 concatemer ($n = 8$) determined at −120 mV. **, $p < 0.01$.

heteromeric channels were also sensitive to CAP. To test whether the heteromeric channels formed by the concatemer vector exhibit altered CAP sensitivity compared with homomeric TRPV1 channels, we measured current amplitudes of homomeric and heteromeric channels in response to different concentrations of CAP (Fig. 2, *A* and *B*). Current responses were normalized to the level at 10 μM CAP, a saturating concentration for both channel types, before being plotted against the CAP concentration (Fig. 2*C*). We noticed that the dose-response curve for the heteromeric channels is much shallower; as a result, the Hill coefficient of heteromeric channels (0.85 ± 0.06) is significantly smaller than that of homomeric TRPV1 (1.88 ± 0.07) ($p < 0.001$) (Fig. 2*D, left panel*). To confirm that the difference in Hill coefficients was not caused by artificial changes in channel function due to the covalent linkage between subunits, we compared the capsaicin dose-response relationships of channels formed by a TRPV1-TRPV1 concatemer to those formed by the TRPV1 monomer. We found these homomeric channels exhibited similar Hill coefficients (Fig. 2*D*, *left panel*). Given that the heteromeric channels contain only two diagonally arranged CAP-binding sites, compared with four binding sites in homomeric TRPV1, the results could be easily explained by a reduced number of CAP-binding sites (Fig. 2*F*). A possible decreased level of cooperativity between TRPV1 subunits because of spatial separation could also contribute to the shallower slope.

We observed that the EC_{50} value of heteromeric channels (269 ± 27 nM) is smaller than that of homomeric TRPV1 (981 ± 59 nM) ($p < 0.001$) (Fig. 2, *C* and *D*). Again, channels formed by the TRPV1-TRPV1 concatemer behaved similarly to channels formed by the TRPV1 monomer (Fig. 2*D*, *right panel*). This finding implicates that physiologically the heteromeric channels may be more sensitive to chemical stimuli.

We further examined the maximal activation level of TRPV1 homomeric channels and heteromeric TRPV1-TRPV3 channels at saturating capsaicin concentrations. Single channel recordings showed that 10 μM capsaicin could activate TRPV1 homomeric channels to a near unity open probability (Fig. 2*E*). At the same capsaicin concentration, homomeric channels formed by the TRPV1-TRPV1 concatemer also reached near unity open probability (data not shown). However, capsaicin could only partially activate the TRPV1-TRPV3 heteromeric channels ($P_o = 61.3 \pm 5.6\%$, $n = 4$) (Fig. 2*E*). This lower efficacy is most likely due to the much reduced chemical energy that drives channel activation (two capsaicin bindings per channel *versus* four bindings).

To corroborate findings from capsaicin activation, we examined the inhibition effects of CZP, a TRPV1-specific antagonist. Despite similar voltage-dependent activations between the heteromeric channels and the homomers (Fig. 3), CZP caused a significant shift of the half-activation voltage of the heteromer to a more depolarized range (Fig. 4, *A–D*). Moreover, measuring from the time course of current inhibition upon CZP application, the heteromers had a reduced on rate and an increased off rate (Fig. 4, *E* and *F*). These changes indicate that indeed heteromeric channels have altered ligand sensitivities and likely a reduced level of cooperativity.

Heteromeric TRPV1/TRPV3 Channels Share the Same Pore—In a Ca^{2+} assay, we found that expression of the TRPV1-TRPV3 concatemer led to a larger rise of the intracellular Ca^{2+} concentration, $[Ca^{2+}]_i$, in response to CAP (Fig. 5*A*) than the expression of TRPV1 alone. Previous studies have established that

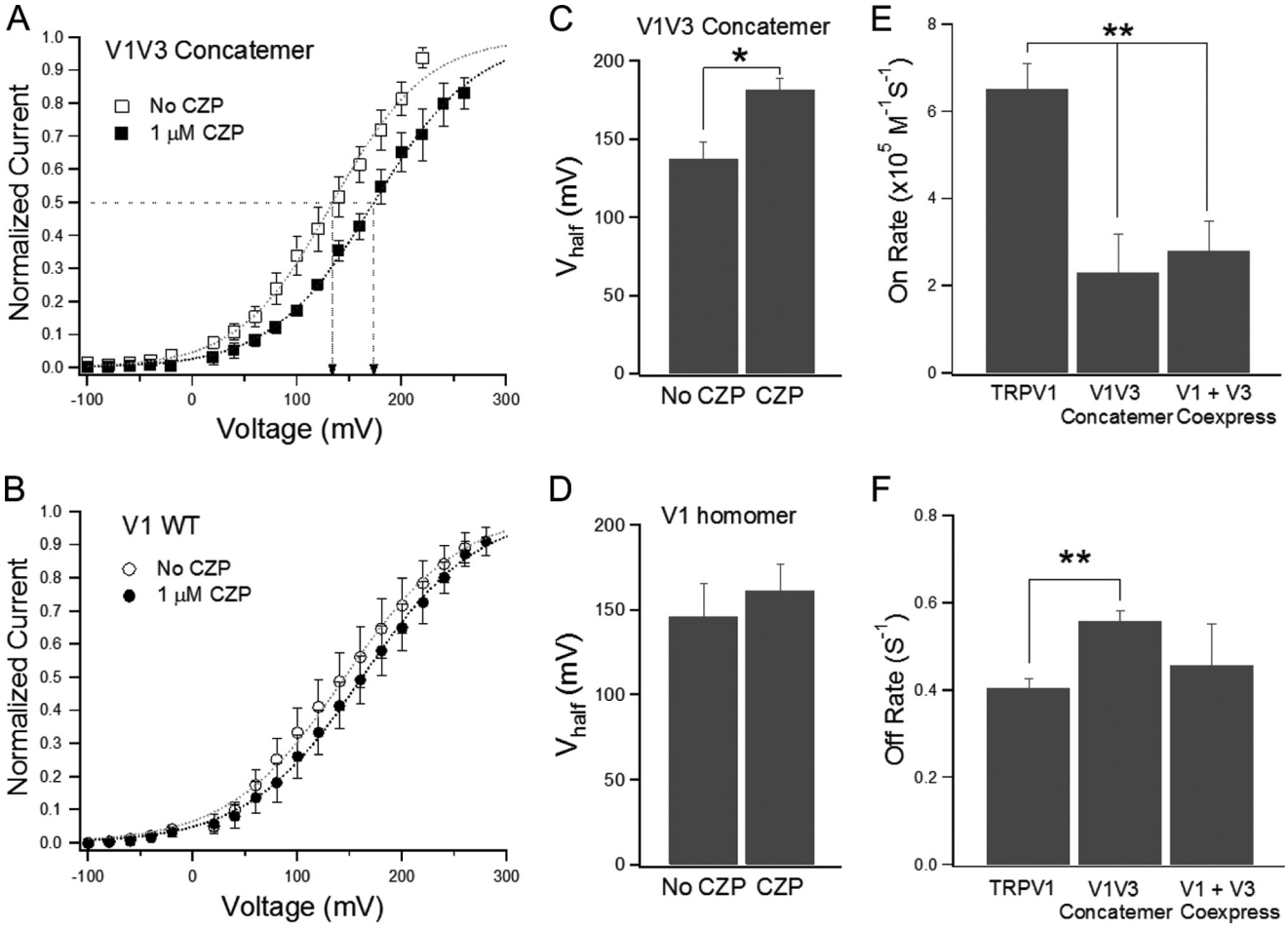

FIGURE 4. **Shifts in voltage dependence caused by capsazepine.** *A* and *B*, *G-V* curves of TRPV1-TRPV3 concatemer and homomeric TRPV1, respectively, in the presence or absence of 1 μM capsazepine. *Dotted curves* represent fits of a Boltzmann function to data points. *Dotted lines* with an *arrowhead* in *A* indicate the V_{half} values. *C* and *D*, V_{half} values of TRPV1-TRPV3 concatemer and homomeric TRPV1, respectively (n = 3–7). *E* and *F*, capsazepine on and off rates for homomeric TRPV1, TRPV1-TRPV3 concatemer, and TRPV1 + TRPV3 co-expression (n = 3–9). *, $p < 0.05$; **, $p < 0.01$.

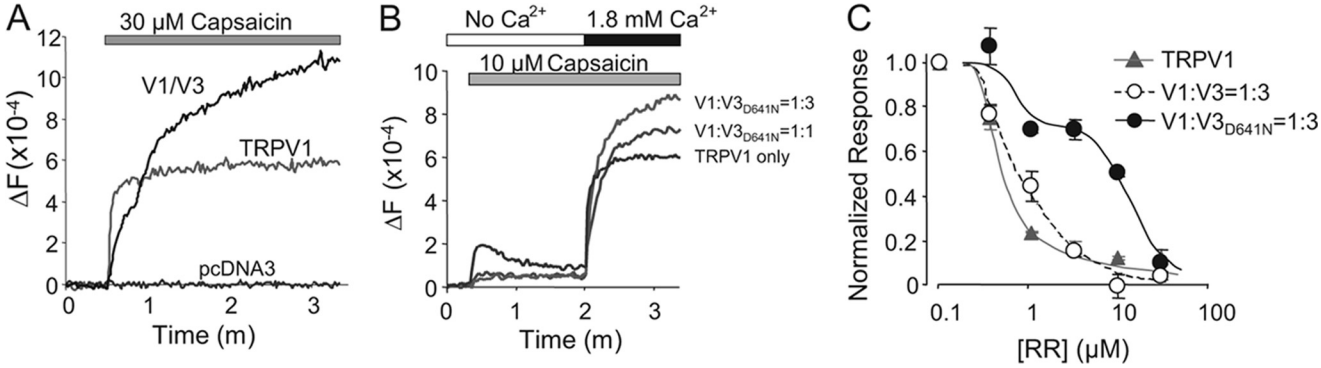

FIGURE 5. **Heteromeric TRPV1/TRPV3 channels share the same conducting pore.** *A*, capsaicin-induced increases in intracellular Ca^{2+} concentration ($[Ca^{2+}]_i$) in cells expressing TRPV1 and TRPV1/TRPV3 concatemer. pcDNA3 was transfected as a negative control. *B*, co-expression of TRPV1 and $TRPV3_{D641N}$ caused a decrease in capsaicin-induced Ca^{2+} release and an increase in the agonist-induced Ca^{2+} influx. *C*, co-expression with $TRPV3_{D641N}$, but not the wild type TRPV3, decreased the RR sensitivity of the capsaicin-induced Ca^{2+} response.

Asp-641 at the pore loop of TRPV3 is critical for the sensitivity to extracellular Ca^{2+} and the nonspecific TRPV channel blocker, ruthenium red (RR) (27, 28). The substitution of Asp-641 by Asn ($TRPV3_{D641N}$) led to a substantial decrease (>100-fold) of channel sensitivity to RR. We reasoned that if TRPV1 and TRPV3 co-assemble to form a conducting pore, it should share properties unique to each of the participating subunits. Thus, co-assembly of TRPV1 and $TRPV3_{D641N}$, but not the wild type TRPV3, should display decreased RR sensitivity of CAP-induced response. Monitoring CAP-induced changes in $[Ca^{2+}]_i$, we found that similar to the TRPV1/TRPV3 concatemer, cells co-expressing TRPV1 and $TRPV3_{D641N}$ gave rise to a larger $[Ca^{2+}]_i$ rise than cells expressing TRPV1 alone, and the increase was correlated with the relative amount of $TRPV3_{D641N}$ cDNA for co-expression (Fig. 5*B*). These observations suggest that the heteromeric channels were indeed

formed in co-expressing cells and that the heteromeric channels appeared to be more Ca^{2+}-permeable. The finding is consistent with the fact that TRPV3 has a higher Ca^{2+} permeability ($P_{Ca}/P_{Na} = 12.1$) than TRPV1 ($P_{Ca}/P_{Na} = 9.6$) (29) as well as a higher single channel conductance (Fig. 1, *B* and *C*) (21), indicating that the heteromeric channel inherited these permeation properties. Furthermore, as expected, a right shift in RR sensitivity of the CAP-induced $[Ca^{2+}]_i$ was observed with cells that co-expressed TRPV1 and $TRPV3_{D641N}$ but not with cells co-expressing TRPV1 and TRPV3 (Fig. 5*C*). Because the CAP sensitivity is encoded by TRPV1 and the low RR sensitivity is encoded by $TRPV3_{D641N}$, this result can only be interpreted as the co-assembled channel having properties of both subunits. Because the RR sensitivity site is situated at the mouth of the conducting pore, the result is consistent with the expectation that the co-assembled pore is composed of pore loops from both TRPV1 and $TRPV3_{D641N}$.

Altered Heat Activation Threshold of Heteromeric TRPV1/TRPV3 Channels—It is well known that heat-sensitive TRPV channels possess distinct temperature thresholds, beyond which the channel starts to respond to temperature change with very high sensitivity. TRPV1 is activated by noxious heat, whereas TRPV3 is activated at innocuous warm temperatures. If heat activation of the TRPV3 subunits is sufficient to open the heteromeric TRPV1/TRPV3 channels, one would expect that the heteromeric channels exhibit a temperature threshold similar to that of TRPV3 and lower than that of TRPV1. Conversely, if activation of all four subunits is required to open the heteromeric channels, the temperature threshold would be similar to that of TRPV1. To distinguish these scenarios, we measured the heat-induced current from inside-out patches (Fig. 6*A*). Surprisingly, we observed that for heteromeric channels generated from either the TRPV1-TRPV3 concatemer or co-expression of TRPV1 and TRPV3 subunits, the temperature thresholds were around 33 °C (33.3 ± 0.6 °C, $n = 10$, and 33.7 ± 0.4 °C, $n = 6$, respectively), which were between those of TRPV1 (37.7 ± 0.3 °C, $n = 9$) and TRPV3 (31.3 ± 0.6 °C, $n = 7$) (Fig. 6*B*). Again, homomeric TRPV1 channels formed by the TRPV1-TRPV1 concatemer behaved very similarly to homomeric TRPV1 channels formed by the TRPV1 monomer (Fig. 6). The heat activation threshold analysis again suggests that the TRPV1 and TRPV3 subunits must interact with each other in the heteromers during heat activation.

Altered Heat Activation Kinetics of Heteromeric TRPV1/TRPV3 Channels—For heat-sensitive TRPV channels, heat activation kinetics is another important functional property. TRPV3 activates slowly whereas heat activation of TRPV1 is rapid (Fig. 7*A*). We characterized the activation kinetics of the heteromeric channels. To ensure that the rate of temperature change was much faster than the rate of channel activation, we employed a laser heating method (25) to heat the patch pipette tip above 45 °C in less than 30 ms. Recording from inside-out patches held at +80 mV, we observed that the heteromeric channels and the homomers exhibit marked differences in the activation rate in response to heating (Fig. 7*A*). We noticed that although TRPV1 showed the fastest heat activation kinetics (time constant around 50 ms), the rate was still slower than the rate of temperature increase, which validates the laser heating approach. As shown in Fig. 7*B*, the heat activation rates of the heteromeric channels, formed either by co-expression or the concatemer, were intermediate of the rates of homomeric TRPV1 and TRPV3. This observation indicates that interaction between TRPV1 and TRPV3 subunits may slow down or speed up the activation rate of individual subunits.

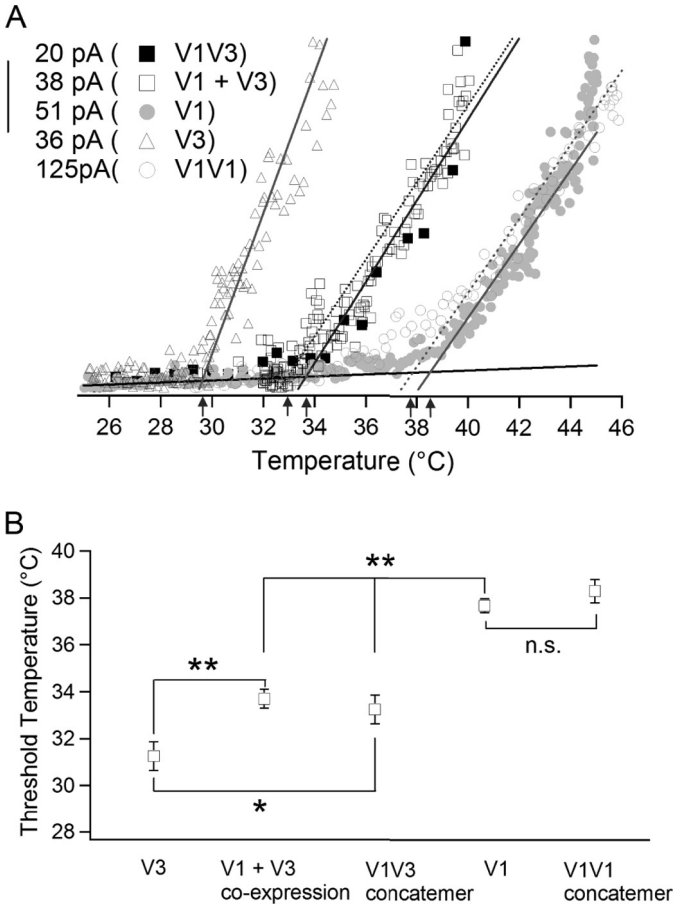

FIGURE 6. **TRPV1, TRPV3, and heteromeric TRPV1/TRPV3 channels exhibit distinct heat activation thresholds.** *A*, representative heat activation time courses recorded at 80 mV. The temperature threshold is defined as the intersection (*arrows*) of the pair of fitted linear functions to the leak current and the heat-activated channel current. *B*, comparison of the measured temperature threshold values of homomeric TRPV1 (37.7 ± 0.3 °C, $n = 9$), TRPV1-TRPV1 concatemer (38.3 ± 0.5 °C, $n = 6$), TRPV3 (31.3 ± 0.6 °C, $n = 7$), TRPV1 + TRPV3 co-expression (33.7 ± 0.4 °C, $n = 6$), and TRPV1-TRPV3 concatemer (33.3 ± 0.6 °C, $n = 10$). *, $p < 0.05$; **, $p < 0.01$; *n.s.*, not significant.

To better understand the differences in their heat activation kinetics, we measured the activation rates of TRPV1 and the heteromer formed by the concatemer at different temperatures (Fig. 7*C*). By fitting the data sets to the Arrhenius equation, we calculated the activation energy (E_a). For heteromeric channels, the value (24.4 ± 3.3 kcal/mol, $n = 3–4$) was much smaller than that of TRPV1 (58.0 ± 5.0 kcal/mol, $n = 4–6$). The reduced E_a implies that the energy barrier for heat activation of heteromeric channels is much lowered.

Altered Heat-induced Potentiation of Heteromeric TRPV1/TRPV3 Channels—Heat-dependent potentiation provides another way to fine tune the physiological properties of heat-activated TRPV channels. Under our experimental conditions (cell-free patches recorded in the absence of Ca^{2+}), TRPV1 exhibited virtually no heat-dependent potentiation (Fig. 8*A*),

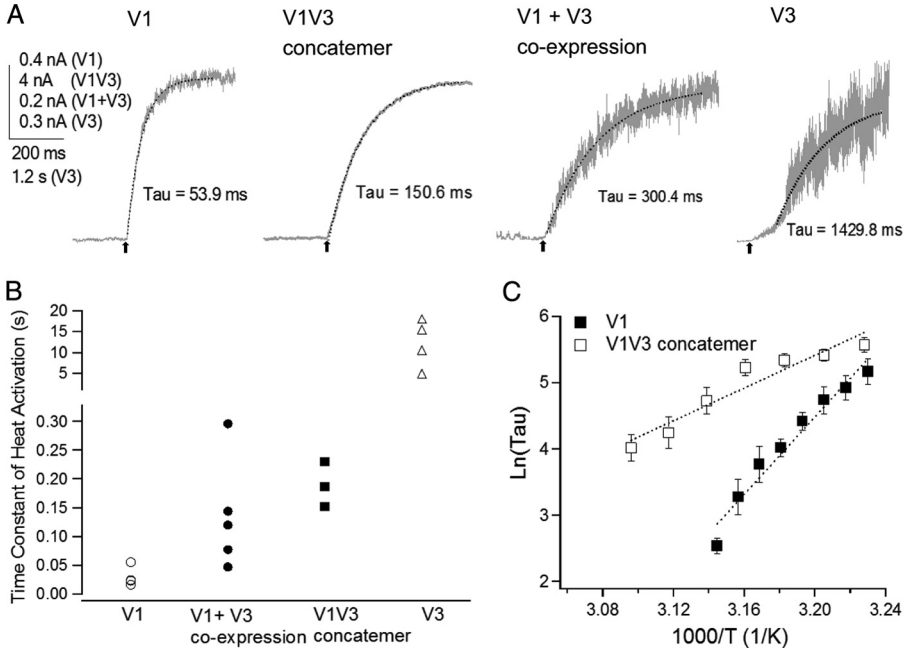

FIGURE 7. **TRPV1, TRPV3, and heteromeric TRPV1/TRPV3 channels exhibit distinct heat activation kinetics.** *A*, representative current traces at +80 mV elicited by rapid laser heating (TRPV1, TRPV1 + TRPV3 co-expression, and TRPV1-TRPV3 concatemer) or by perfusion (TRPV3, because of its slow activation time course). A single exponential function is used to fit to the current raising phase (*dotted curve*) from which the time constant of heat activation is estimated. *B*, distribution of heat activation time constants. Values for TRPV1, TRPV1 + TRPV3 co-expression, and TRPV1-TRPV3 concatemer are measured from current responses to heating at 43 °C; those of TRPV3 are measured at 37 °C. Each *symbol* represents an individual measurement. *C*, temperature dependence of heat activation time constants of TRPV1 ($n = 4–6$ for each temperature level) and TRPV1/TRPV3 concatemer ($n = 3–4$). *Dotted lines* represent fits to the Arrhenius equation.

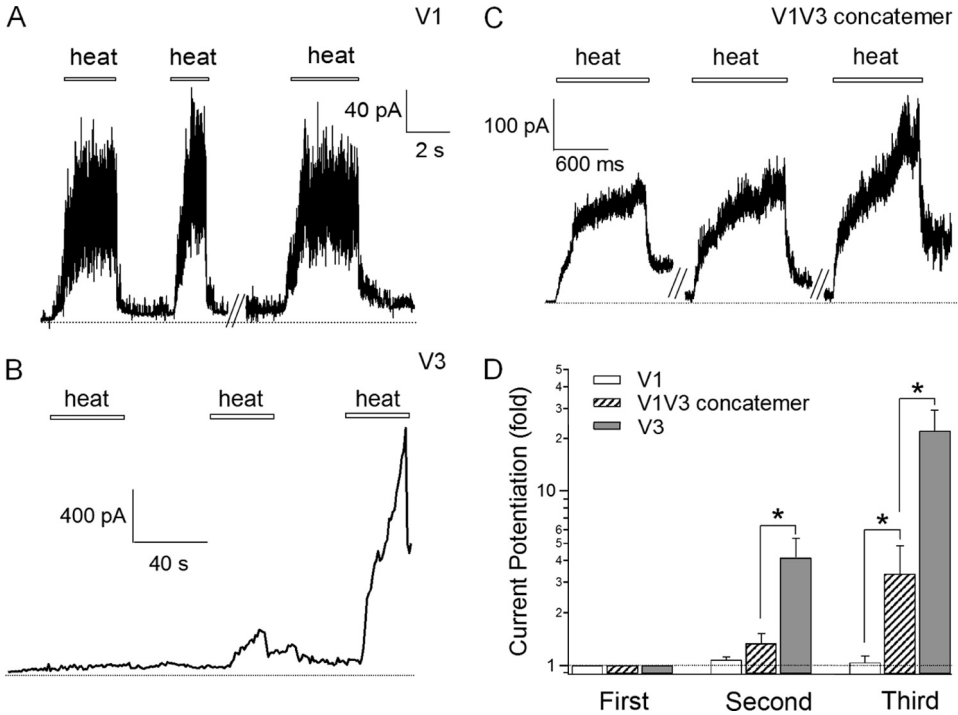

FIGURE 8. **Potentiation of TRPV1, TRPV3, and heteromeric TRPV1/TRPV3 channel by repetitive heating.** *A–C*, representative current responses of homomeric TRPV1, homomeric TRPV3, and TRPV1/TRPV3 concatemer, respectively, to repeated heating up to 40 °C. *D*, fold change in current amplitude upon repeated heating ($n = 3–8$). *, $p < 0.05$.

although the current response of TRPV3 could be substantially enhanced by repetitive heating (Fig. 8*B*). The difference reflects an intrinsic difference in the gating properties of TRPV1 and TRPV3 subunits, which contributes toward shaping the channel activation profile (27). For heteromeric channels, we observed significant current potentiation upon repeated heating; however, the magnitude of current increase was much smaller than that of TRPV3 (Fig. 8, *C* and *D*), suggesting again substantial interaction between TRPV1 and TRPV3 subunits during gating.

DISCUSSION

In this study we systematically investigated the functional properties of heteromeric TRPV1/TRPV3 channels activated by heat, agonists and antagonists, and voltage. Our results demonstrated that the heteromeric channels are different from homomeric channels in sensitivities and dynamic range to thermal and chemical stimuli but to a much less extent to changes in transmembrane voltage; they also show potentiation by repetitive heat stimuli. These observations indicate that they serve as distinct cellular sensors to thermal and chemical stimuli and are thus expected to mediate different sensory responses to benign and noxious environmental cues. That co-expression of TRPV1 with a TRPV3 mutant with reduced RR sensitivity resulted in reduced sensitivity of CAP-induced $[Ca^{2+}]_i$ to RR strongly argues for the shared pore architecture between the TRPV1 and TRPV3 subunits in the assembled channel. Our data further indicated that subunit-subunit interactions underlie the distinct gating behaviors in heteromeric channels. Like other multisubunit channels, temperature-sensitive TRP channels are known to be allosteric proteins (30). Cooperative gating among subunits shifts the sensitivity and dynamic range exhibited by subunits in homomeric channels, sometimes in unexpected ways (such as to the capsaicin sensitivity). These properties must be carefully considered when examining the response of native neurons to heat and agonists.

Recently we reported that a tetramerization assembly domain in the intracellular C terminus helps to mediate the assembly of homomeric TRPV1–4 channels (31). We speculate that a similar mechanism may also contribute to heteromeric subunit assembly. Initial pulldown assays indeed demonstrated that the C termini of TRPV1 and TRPV3 interact *in vitro*, whereas negative controls using the same C-terminal constructs under similar conditions did not show any nonspecific interaction with GST proteins (data not shown). As the intracellular C terminus of various TRPV channels is known to participate in the activation conformational changes (32–36), the interaction between tetramerization assembly domains might contribute to changes in cooperativity in heteromeric TRPV channels as observed in the functional tests. Future experiments will be needed to fully test this possibility.

Experimental investigation of the physiological roles of thermosensitive TRP channels has been done so far mostly with rodents. Recent studies, however, highlighted the limitation of using animal models in understanding human physiology (19, 20). Capsaicin receptors in human sensory neurons exhibit significant heterogeneity that might reflect differences in the subunit composition (37). The capsaicin response of adult human dorsal root ganglion (DRG) neurons in culture has an apparent EC_{50} of 160 nM (38), which is closer to the EC_{50} value for heteromeric channels and much lower than that of the homomeric TRPV1 channels (see also Fig. 2*C*). Indeed, it is known that TRPV1 co-expresses with other temperature-sensitive TRP channels in DRG neurons (39–41). In particular, co-expression of TRPV1 and TRPV3 in human DRG neurons is well documented (14, 42). Whereas the rodent DRG neurons apparently lack TRPV3 (13), the human TRPV3 was originally cloned from DRG neurons (14, 15). The functional differences between homomeric and heteromeric channels should contribute to the physiological properties of native neurons in both Ca^{2+} influx and membrane excitability.

Expression of TRP channels in native tissues is dynamically regulated by both developmental and environmental cues (43–45). Of particular clinical importance is the induced overexpression of TRPV channels under pathological conditions such as traumatic and diabetic neuropathy, tissue injury, and inflammation (11, 14, 40, 42, 46–48). Such dynamic changes have been suggested to contribute to elevated sensitivity to noxious stimuli as seen in hyperalgesia. The distributions of TRPV1–4 channels overlap extensively in both neuronal and non-neuronal tissues. It thus seems likely that the formation of heteromeric TRPV channels of diverse functionalities can also be dynamically regulated, resulting in fine-tuning of the cellular response to environmental changes.

Acknowledgments—We thank Sharona Gordon and Ardem Patapoutian for providing cDNA of TRPV3 and current and previous laboratory members for assistance and discussions.

REFERENCES

1. Clapham, D. E. (2002) Signal transduction. Hot and cold TRP ion channels. *Science* **295,** 2228–2229
2. Jordt, S. E., McKemy, D. D., and Julius, D. (2003) Lessons from peppers and peppermint. The molecular logic of thermosensation. *Curr. Opin. Neurobiol.* **13,** 487–492
3. Bandell, M., Macpherson, L. J., and Patapoutian, A. (2007) From chills to chilis. Mechanisms for thermosensation and chemesthesis via thermoTRPs. *Curr. Opin. Neurobiol.* **17,** 490–497
4. Yang, F., Cui, Y., Wang, K., and Zheng, J. (2010) Thermosensitive TRP channel pore turret is part of the temperature activation pathway. *Proc. Natl. Acad. Sci. U.S.A.* **107,** 7083–7088
5. Latorre, R., Zaelzer, C., and Brauchi, S. (2009) Structure-functional intimacies of transient receptor potential channels. *Q. Rev. Biophys.* **42,** 201–246
6. Moiseenkova-Bell, V. Y., Stanciu, L. A., Serysheva, I. I., Tobe, B. J., and Wensel, T. G. (2008) Structure of TRPV1 channel revealed by electron cryomicroscopy. *Proc. Natl. Acad. Sci. U.S.A.* **105,** 7451–7455
7. Mosavi, L. K., Cammett, T. J., Desrosiers, D. C., and Peng, Z. Y. (2004) The ankyrin repeat as molecular architecture for protein recognition. *Protein Sci.* **13,** 1435–1448
8. Sedgwick, S. G., and Smerdon, S. J. (1999) The ankyrin repeat. A diversity of interactions on a common structural framework. *Trends Biochem. Sci.* **24,** 311–316
9. Rohács, T., Lopes, C. M., Michailidis, I., and Logothetis, D. E. (2005) $PI(4,5)P_2$ regulates the activation and desensitization of TRPM8 channels through the TRP domain. *Nat. Neurosci.* **8,** 626–634
10. Caterina, M. J., Schumacher, M. A., Tominaga, M., Rosen, T. A., Levine, J. D., and Julius, D. (1997) The capsaicin receptor. A heat-activated ion channel in the pain pathway. *Nature* **389,** 816–824
11. Caterina, M. J., Leffler, A., Malmberg, A. B., Martin, W. J., Trafton, J., Petersen-Zeitz, K. R., Koltzenburg, M., Basbaum, A. I., and Julius, D. (2000) Impaired nociception and pain sensation in mice lacking the capsaicin receptor. *Science* **288,** 306–313
12. Yan, T., Liu, B., Du, D., Eisenach, J. C., and Tong, C. (2007) Estrogen amplifies pain responses to uterine cervical distension in rats by altering transient receptor potential-1 function. *Anesth. Analg.* **104,** 1246–1250
13. Peier, A. M., Reeve, A. J., Andersson, D. A., Moqrich, A., Earley, T. J., Hergarden, A. C., Story, G. M., Colley, S., Hogenesch, J. B., McIntyre, P., Bevan, S., and Patapoutian, A. (2002) A heat-sensitive TRP channel expressed in keratinocytes. *Science* **296,** 2046–2049
14. Smith, G. D., Gunthorpe, M. J., Kelsell, R. E., Hayes, P. D., Reilly, P., Facer,

P., Wright, J. E., Jerman, J. C., Walhin, J. P., Ooi, L., Egerton, J., Charles, K. J., Smart, D., Randall, A. D., Anand, P., and Davis, J. B. (2002) TRPV3 is a temperature-sensitive vanilloid receptor-like protein. *Nature* **418,** 186–190
15. Xu, H., Ramsey, I. S., Kotecha, S. A., Moran, M. M., Chong, J. A., Lawson, D., Ge, P., Lilly, J., Silos-Santiago, I., Xie, Y., DiStefano, P. S., Curtis, R., and Clapham, D. E. (2002) TRPV3 is a calcium-permeable temperature-sensitive cation channel. *Nature* **418,** 181–186
16. Macpherson, L. J., Hwang, S. W., Miyamoto, T., Dubin, A. E., Patapoutian, A., and Story, G. M. (2006) More than cool. Promiscuous relationships of menthol and other sensory compounds. *Mol. Cell. Neurosci.* **32,** 335–343
17. Xu, H., Delling, M., Jun, J. C., and Clapham, D. E. (2006) Oregano, thyme, and clove-derived flavors and skin sensitizers activate specific TRP channels. *Nat. Neurosci.* **9,** 628–635
18. Gunthorpe, M. J., Benham, C. D., Randall, A., and Davis, J. B. (2002) The diversity in the vanilloid (TRPV) receptor family of ion channels. *Trends Pharmacol. Sci.* **23,** 183–191
19. Huang, S. M., Li, X., Yu, Y., Wang, J., and Caterina, M. J. (2011) TRPV3 and TRPV4 ion channels are not major contributors to mouse heat sensation. *Mol. Pain* **7,** 37
20. Moqrich, A., Hwang, S. W., Earley, T. J., Petrus, M. J., Murray, A. N., Spencer, K. S., Andahazy, M., Story, G. M., and Patapoutian, A. (2005) Impaired thermosensation in mice lacking TRPV3, a heat and camphor sensor in the skin. *Science* **307,** 1468–1472
21. Cheng, W., Yang, F., Takanishi, C. L., and Zheng, J. (2007) Thermosensitive TRPV channel subunits co-assemble into heteromeric channels with intermediate conductance and gating properties. *J. Gen. Physiol.* **129,** 191–207
22. Cheng, W., Sun, C., and Zheng, J. (2010) Heteromerization of TRP channel subunits: extending functional diversity. *Protein Cell* **1,** 802–810
23. Colton, C. K. (2006) *TRPV3 Is a Polymodal Receptor.* Ph.D. thesis, Ohio State University, Columbus
24. Wang, C., Hu, H. Z., Colton, C. K., Wood, J. D., and Zhu, M. X. (2004) An alternative splicing product of the murine *trpv1* gene dominant negatively modulates the activity of TRPV1 channels. *J. Biol. Chem.* **279,** 37423–37430
25. Liang, S., Yang, F., Zhou, C., Wang, Y., Li, S., Sun, C. K., Puglisi, J. L., Bers, D., Sun, C., and Zheng, J. (2009) Temperature-dependent activation of neurons by continuous near-infrared laser. *Cell Biochem. Biophys.* **53,** 33–42
26. Isacoff, E. Y., Jan, Y. N., and Jan, L. Y. (1990) Evidence for the formation of heteromultimeric potassium channels in *Xenopus* oocytes. *Nature* **345,** 530–534
27. Chung, M. K., Güler, A. D., and Caterina, M. J. (2005) Biphasic currents evoked by chemical or thermal activation of the heat-gated ion channel, TRPV3. *J. Biol. Chem.* **280,** 15928–15941
28. Xiao, R., Tang, J., Wang, C., Colton, C. K., Tian, J., and Zhu, M. X. (2008) Calcium plays a central role in the sensitization of TRPV3 channel to repetitive stimulations. *J. Biol. Chem.* **283,** 6162–6174
29. Benham, C. D., Gunthorpe, M. J., and Davis, J. B. (2003) TRPV channels as temperature sensors. *Cell Calcium* **33,** 479–487
30. Latorre, R., Brauchi, S., Orta, G., Zaelzer, C., and Vargas, G. (2007) ThermoTRP channels as modular proteins with allosteric gating. *Cell Calcium* **42,** 427–438
31. Zhang, F., Liu, S., Yang, F., Zheng, J., and Wang, K. (2011) Identification of a tetrameric assembly domain in the C terminus of heat-activated TRPV1 channels. *J. Biol. Chem.* **286,** 15308–15316
32. Vlachová, V., Teisinger, J., Susánková, K., Lyfenko, A., Ettrich, R., and Vyklický, L. (2003) Functional role of C-terminal cytoplasmic tail of rat vanilloid receptor 1. *J. Neurosci.* **23,** 1340–1350
33. Brauchi, S., Orta, G., Salazar, M., Rosenmann, E., and Latorre, R. (2006) A hot-sensing cold receptor: C-terminal domain determines thermosensation in transient receptor potential channels. *J. Neurosci.* **26,** 4835–4840
34. Brauchi, S., Orta, G., Mascayano, C., Salazar, M., Raddatz, N., Urbina, H., Rosenmann, E., Gonzalez-Nilo, F., and Latorre, R. (2007) Dissection of the components for PIP_2 activation and thermosensation in TRP channels. *Proc. Natl. Acad. Sci. U.S.A.* **104,** 10246–10251
35. Valente, P., García-Sanz, N., Gomis, A., Fernández-Carvajal, A., Fernández-Ballester, G., Viana, F., Belmonte, C., and Ferrer-Montiel, A. (2008) Identification of molecular determinants of channel gating in the transient receptor potential box of vanilloid receptor I. *FASEB J.* **22,** 3298–3309
36. García-Sanz, N., Valente, P., Gomis, A., Fernández-Carvajal, A., Fernández-Ballester, G., Viana, F., Belmonte, C., and Ferrer-Montiel, A. (2007) A role of the transient receptor potential domain of vanilloid receptor I in channel gating. *J. Neurosci.* **27,** 11641–11650
37. Szallasi, A. (1995) Autoradiographic visualization and pharmacological characterization of vanilloid (capsaicin) receptors in several species, including man. *Acta Physiol. Scand. Suppl.* **629,** 1–68
38. Baumann, T. K., Burchiel, K. J., Ingram, S. L., and Martenson, M. E. (1996) Responses of adult human dorsal root ganglion neurons in culture to capsaicin and low pH. *Pain* **65,** 31–38
39. Greffrath, W., Binzen, U., Schwarz, S. T., Saaler-Reinhardt, S., and Treede, R. D. (2003) Co-expression of heat sensitive vanilloid receptor subtypes in rat dorsal root ganglion neurons. *Neuroreport* **14,** 2251–2255
40. Jordt, S. E., Bautista, D. M., Chuang, H. H., McKemy, D. D., Zygmunt, P. M., Högestätt, E. D., Meng, I. D., and Julius, D. (2004) Mustard oils and cannabinoids excite sensory nerve fibers through the TRP channel ANKTM1. *Nature* **427,** 260–265
41. Story, G. M., Peier, A. M., Reeve, A. J., Eid, S. R., Mosbacher, J., Hricik, T. R., Earley, T. J., Hergarden, A. C., Andersson, D. A., Hwang, S. W., McIntyre, P., Jegla, T., Bevan, S., and Patapoutian, A. (2003) ANKTM1, a TRP-like channel expressed in nociceptive neurons, is activated by cold temperatures. *Cell* **112,** 819–829
42. Facer, P., Casula, M. A., Smith, G. D., Benham, C. D., Chessell, I. P., Bountra, C., Sinisi, M., Birch, R., and Anand, P. (2007) Differential expression of the capsaicin receptor TRPV1 and related novel receptors TRPV3, TRPV4, and TRPM8 in normal human tissues and changes in traumatic and diabetic neuropathy. *BMC Neurol.* **7,** 11
43. Hjerling-Leffler, J., Alqatari, M., Ernfors, P., and Koltzenburg, M. (2007) Emergence of functional sensory subtypes as defined by transient receptor potential channel expression. *J. Neurosci.* **27,** 2435–2443
44. Puntambekar, P., Mukherjea, D., Jajoo, S., and Ramkumar, V. (2005) Essential role of Rac1/NADPH oxidase in nerve growth factor induction of TRPV1 expression. *J. Neurochem.* **95,** 1689–1703
45. Vetter, I., Cheng, W., Peiris, M., Wyse, B. D., Roberts-Thomson, S. J., Zheng, J., Monteith, G. R., and Cabot, P. J. (2008) Rapid, opioid-sensitive mechanisms involved in transient receptor potential vanilloid 1 sensitization. *J. Biol. Chem.* **283,** 19540–19550
46. Gopinath, P., Wan, E., Holdcroft, A., Facer, P., Davis, J. B., Smith, G. D., Bountra, C., and Anand, P. (2005) Increased capsaicin receptor TRPV1 in skin nerve fibers and related vanilloid receptors TRPV3 and TRPV4 in keratinocytes in human breast pain. *BMC Womens Health* **5,** 2
47. Siemens, J., Zhou, S., Piskorowski, R., Nikai, T., Lumpkin, E. A., Basbaum, A. I., King, D., and Julius, D. (2006) Spider toxins activate the capsaicin receptor to produce inflammatory pain. *Nature* **444,** 208–212
48. Bandell, M., Story, G. M., Hwang, S. W., Viswanath, V., Eid, S. R., Petrus, M. J., Earley, T. J., and Patapoutian, A. (2004) Noxious cold ion channel TRPA1 is activated by pungent compounds and bradykinin. *Neuron* **41,** 849–857